Carbohydrate Polymers 251 (2021) 117008

Contents lists available at ScienceDirect

Carbohydrate Polymers

journal homepage: www.elsevier.com/locate/carbpol

A targeted and redox/pH-responsive chitosan oligosaccharide derivatives based nanohybrids for overcoming multidrug resistance of breast cancer cells

Lejiao Jia [a,*], Zhenyu Li [b], Dandan Zheng [c], Zhiying Li [c], Zhongxi Zhao [c,*]

[a] Department of Pharmacy, Qilu Hospital, Cheeloo College of Medicine, Shandong University, Jinan, 250013, China
[b] Department of Pharmacy, Shandong Provincial Hospital Affiliated to Shandong First Medical University, Jinan, 250021, China
[c] School of Pharmaceutical Sciences, Cheeloo College of Medicine, Shandong University, Jinan, 250012, China

ARTICLE INFO

Keywords:
chitosan oligosaccharide
nanoparticles
pH/redox-responsive
co-delivery
multidrug resistance

ABSTRACT

A novel folic acid mediated chitosan oligosaccharide-grafted disulfide-containing polyethylenimine copolymer-based silica nanohybrids were fabricated for co-delivering paclitaxel and P-shRNA. These nanoparticles could efficiently protect P-shRNA against degradation, and exhibited well redox-responsive P-shRNA release and pH-responsive drug release behaviors. Folic acid as the targeting head, could improve cellular uptake of nanoparticles by multidrug-resistant breast cancer cells. Moreover, these nanoparticles showed excellent delivery P-shRNA into cells and displayed high gene silencing efficiency at the targeted mRNAs to downregulate the expression of P-gp which induced up to 63% decrease. Finally, nanoparticles could completely reverse the resistance of breast cancer cells to paclitaxel and the resistance reversion index was 50.59. These results suggested that our nanoparticles could efficiently co-deliver paclitaxel and P-shRNA into cancer cells to exert its synergistic antitumor effect, and opened up a new avenue for overcoming multidrug resistance.

1. Introduction

Multidrug resistance (MDR) is defined as the insensitivity or cross-resistance of cancer cells to the cytostatic/cytotoxic actions of various anticancer drugs, which has become one of the major cause of chemotherapy failure (Baguley, 2010; Bukowski, Kciuk, & Kontek, 2020; Gottesman, Fojo, & Bates, 2002). Two main types of MDR are found in tumors, namely, intrinsic resistance and acquired resistance (Longley & Johnston, 1990). The intrinsic drug resistance is congenitally resistant to chemotherapy and probably associated with the gene mutation or altered expression of BCL-2-related apoptotic proteins (Johnstone, Ruefli, & Lowe, 2002). While, the acquired resistance mainly results from the overexpression of cell membrane-bound ATP-binding cassette (ABC) transporters, usually occurring during the chemotherapy of relapsing leukemia and ovarian, and breast cancers (Pommier, Sordet, Antony, Hayward, & Kohn, 2004). One of the principal transporters is the P-glycoprotein (P-gp) which can efflux out many drugs such as doxorubicin, vinblastine, paclitaxel, and so on, to reduce the intracellular drug concentration below the effective cytotoxic threshold (Holohan, Van Schaeybroeck, Longley, & Johnston, 2013; Mahon et al., 2003; Mizutani et al., 2008). Lots of strategies have been used to overcome MDR, including immunotherapy (Curiel, 2012; Owyong et al., 2017), small-molecule inhibitors (Lai et al., 2019; Snyder, Murundi, Crawford, & Putnam, 2019; Wise et al., 2019), as well as gene therapy (Wang et al., 2019a, 2019b). In all mentioned strategies, short hairpin RNA (shRNA) is a suitable approach owing to that shRNA can mediate transcription of small interfering RNA (siRNA) through a plasmid DNA vector, which offers persistent degradation of a target RNA molecule and knockdown the expression of protein (Oh & Park, 2009; Zheng, Tang, & Yin, 2015). While, labile degradation and lower tumor uptake are obstacles for gene therapy to be applied in clinic (Bartlett & Davis, 2007; Jörg, Baehr, Kiermayer, Zeuzem, & Piiper, 2006). Besides, a great many of antitumor drugs are water-insoluble and lack of targeting which also leads to poor chemotherapy effect and adverse reactions. Hence, it is imperative to discover a prospective carrier to efficiently co-deliver drug and gene agents to tumor regions.

Nowadays, lots of drug carriers have been applied to deliver drugs and/or genes to tumor sites including organic nano-materials, such as lipid nanoparticles, liposomes, nano hydrogels, micelles and polymer nanoparticles (Liu, Anderson, Lan, Conti, & Chen, 2020; Madheswaran,

* Corresponding authors.
E-mail addresses: jialejiao@163.com (L. Jia), zxzhao@sdu.edu.cn (Z. Zhao).

https://doi.org/10.1016/j.carbpol.2020.117008
Received 26 June 2020; Received in revised form 15 August 2020; Accepted 16 August 2020
Available online 2 September 2020
0144-8617/

Kandasamy, Bose, & Karuppagounder, 2019), and inorganic carriers, such as carbon nanomaterials, silica nanoparticles and gold nanoparticles, etc. (Chen et al., 2019; Li et al., 2018; Zhu et al., 2019). Facile silane chemistry offers easy surface modification of silica nanoparticles with plenty of functional groups or organic polymers which makes them highly eligible for multifunctional therapeutic applications (Aquib et al., 2019). Hence, the combination of organic materials and inorganic silica nanoparticles to fabricate hybrid nanoparticles would exhibit enormous superiority for delivering drugs, gene, imaging agents, etc..

Chitosan, consisting of b-(1,4)-linked-2-amino-2-deoxy-D-glucopyranose units, is a natural polysaccharide obtained by chitin, holds potential candidature in gene/drug vehicles since it is nontoxic, biocompatible and biodegradable (Li et al., 2020; Luo et al., 2019; Mu et al., 2019; Qu et al., 2020; Shahidi & Synowiecki, 1991; Wang, Khan et al., 2019; Zhao, Ji, Wang, He, & Li, 2020). However, its high viscosity and poor solubility in physiological pH values (7.2–7.4) are major hurdles on successful application in gene vehicles. Hence, chitosan oligosaccharide (CS), which are products of chitosan depolymerization, has attracted great interest owing to its good water solubility and excellent biocompatibility (Guerry, Cottaz, Fleury, Bernard, & Halila, 2014; Musalli, Talukdar, Roy, Kumar, & Wong, 2020; Wang et al., 2019c). While, due to mild cationic charge densities and proton sponge effect, its application on gene delivery is restricted. CS possess reactive hydroxyl and amino groups, thus further cationic modification is expected to effectively improve the capacity of gene delivery.

Among organic polymers, one of the most potent gene carriers is polyethylenimine (PEI) (Lungwitz, Breunig, Blunk, & Gopferich, 2005). High molecular weight PEI (25 kDa) has been exhibited as the golden standard with high transfection efficiency, however, high toxicity was discovered owing to the lack of degradable linkages in PEI25 K and difficulty to degrade. In contrary, PEI with low molecular weight (LMW PEI) has lower toxicity but almost no transfection activity (Huang, Yu, Tang, Wang, & Li, 2010). To settle this dilemma, in the present study, we choose chitosan oligosaccharide as the polymer backbone to graft LMW PEI using degradable disulfide linkages to construct copolymers with suitable charge density and molecular weights. It is reported that the concentration of GSH in the extracellular environment is quite lower than intracellular GSH (100–1000 times) (Cheng et al., 2011), and hence disulfide linkages in copolymers have good stability outside cells and are cleaved only when internalized by cells. To enhance the colloidal stability and reduce the uptake of the reticuloendothelial system (RES), Poly (ethylene glycol) (PEG) is exploited into our copolymer (Nie, Gunther, Gu, & Wagner, 2011; Nomoto et al., 2011). In order to improve the internalization of nanocarriers by tumor cells, several ligands have been added to the surface of nanoparticles based on overexpressed molecules on the cancer cells surface (Alavi & Hamidi, 2019). In malignancies, including breast cancer, the expression of folate receptors is 20 to 200 times higher than that in normal cell lines (Antony, 1996; Parker et al., 2005). Thus, folic acid (FA) was chosen to graft on our copolymer to enhance selective breast cancer cell uptake. Therefore, we synthesized a novel folic acid mediated chitosan oligosaccharide-grafted disulfide-containing polyethylenimine copolymer copolymers as the gene carrier for delivering shRNA-expressing plasmid DNA for interference with P-glycoprotein (P-shRNA), donated as FA-PEG-CS-PEI.

To overcome drug resistance and achieve optimally synergistic anticancer effects, it is expected to co-deliver P-shRNA and chemotherapeutic drug paclitaxel (PTX) into breast cancer cells by a single nano-vehicle. Cetyltrimethylammonium bromide (CTAB) can form micelles when it was applied as templates to construct silica nanoparticles (Kresge, Leonowicz, Roth, Vartuli, & Beck, 1992). More importantly, in acidic media, CTAB micelles are prone to be destroyed due to positive charges of CTAB exchange with protons (Huo et al., 1994). Therefore, paclitaxel (PTX) can be dispersed into CTAB micelles and silica resources hydrolyzed and condensed to produce PTX-loaded silica nanoparticles (SN). SN could show pH-stimuli release behavior owing to CTAB micelles as the “pH-switch”, which is stable in the neutral environment and destroyed in low pH environment, and then loaded drugs released.

With reference to chitosan or CS derivatives, the late studies exhibit great superiority in delivering siRNA and/or chemotherapeutics (Miao et al., 2019; Musalli et al., 2020; Yin et al., 2020). Compared with siRNA, shRNA could offer persistent degradation of a target RNA via a plasmid DNA vector, however, its large molecular weight (siRNA is commonly only 21 bp) put forward higher request to gene vehicle for protection and delivery. To our acknowledge, a rare research of the chitosan or CS derivatives which can not only successfully co-deliver shRNA and chemotherapeutics, but also exhibit targeted and redox/pH-responsive release cargoes has been reported. Hence, in this study, we innovatively constructed the folic acid grafted CS-grafted disulfide-containing PEI copolymer-based silica nanohybrids (FA-PEG-CS-PEI/SN) for co-delivering P-shRNA and paclitaxel to reverse MDR and enhance chemotherapeutic efficacy in breast cancer cells, as illustrated by Scheme 1. Our hypothesis is as follows: Folic acid as the targeting head, could mediate FA-PEG-CS-PEI/SN to be selective taken up by breast cancer cells. P-shRNA was condensed on the surface via FA-PEG-CS-PEI and drugs can be loaded into the internal channels of nanoparticles through CTAB micelles. Therefore, these hybrid nanoparticles could remain well stable in the blood circulating system. Once endocytosis by tumor cells in the reducing (GSH) intracellular environment, FA-PEG-CS-PEI on the surface of nanoparticles could be disaggregated to fragments of low molecular weight polymers and release DNA cargoes owing to disulfide linkages. Besides, paclitaxel, loaded in the hybrid nanoparticles, exhibited pH-triggered cargo release contributing to that CTAB micelles would be disrupted and loaded drugs released in low pH environment. Thus, our constructed FA-PEG-CS-PEI/SN would possess FA-mediated targeting for breast cancer cells, well pH-sensitive drug release behaviors and excellent GSH response characteristics for releasing P-shRNA to achieve synergistic therapeutic strategy for multidrug resistant breast cancer cells.

2. Experimental Section

2.1. Materials

Paclitaxel (PTX) was obtained from Xi’an Haoxuan. 3,3’-Dithiodipropionic acid was obtained from Tokyo. Chitosan oligosaccharide (Mw = 3000 Da) were obtained from Haidebei Marine. N-hydroxysuccinimide (NHS), 1-Ethyl-3-(3-dime-thylaminopropyl) carbodiimide hydrochloride (EDC), DMSO, MTT, methyl(3-trihydroxysilylpropoxy) phos-phinate, RPMI1640 (free folic acid), folic acid, Anti-β-actin and HRP Goat Anti-Rabbit (IgG) secondary antibody were purchased from Sigma-Aldrich. Tetraethyl orthosilicate (TEOS, 98%), branched polyethylenimine (PEI, Mw = 1800 Da) and Cetyltrimethylammonium bromide (CTAB, 99%) were purchased from Alfa Aesar. mPEG-NH_2 (Mw = 2000 Da) and NH_2-PEG-NH_2 (Mw = 2000 Da) were obtained from Aladdin. Dnase I, glutathione (GSH) and heparin were purchased from Roche. Anti-P Glycoprotein antibody was purchased from Abcam. Ammonium fluoride Fluorescein isothiocyanate (FITC) was obtained from Klontech. (NH_4F, 96%) was purchased from Sinopharm. SanPrep Column Plasmid Mini-Preps Kit was provided by Sangon Biotech. 0.25% (w/v) trypsin solution, penicilline-streptomycin and RPMI1640, fetal bovine serum (FBS) were purchased from Gibco. First Strand cDNA Synthesis Kit was purchased from Fermentas. Annexin V-FITC Apoptosis Detection kit was provided by KeyGen. The protein Marker (with molecular weight of 11-245 KD) was provided by Solarbio.

Cell culture: Human breast cancer MCF-7 cell and its multidrug-resistant cell (MCF-7/ADR) were cultured in RPMI1640 medium (free folic acid), supplemented with 10% FBS,100 U/mL of penicillin and 100 mg/mL of streptomycin. All cells were cultured in incubators maintained at 37 °C with 5% CO_2 under fully humidified conditions. All experiments were performed on cells in the logarithmic phase of growth.

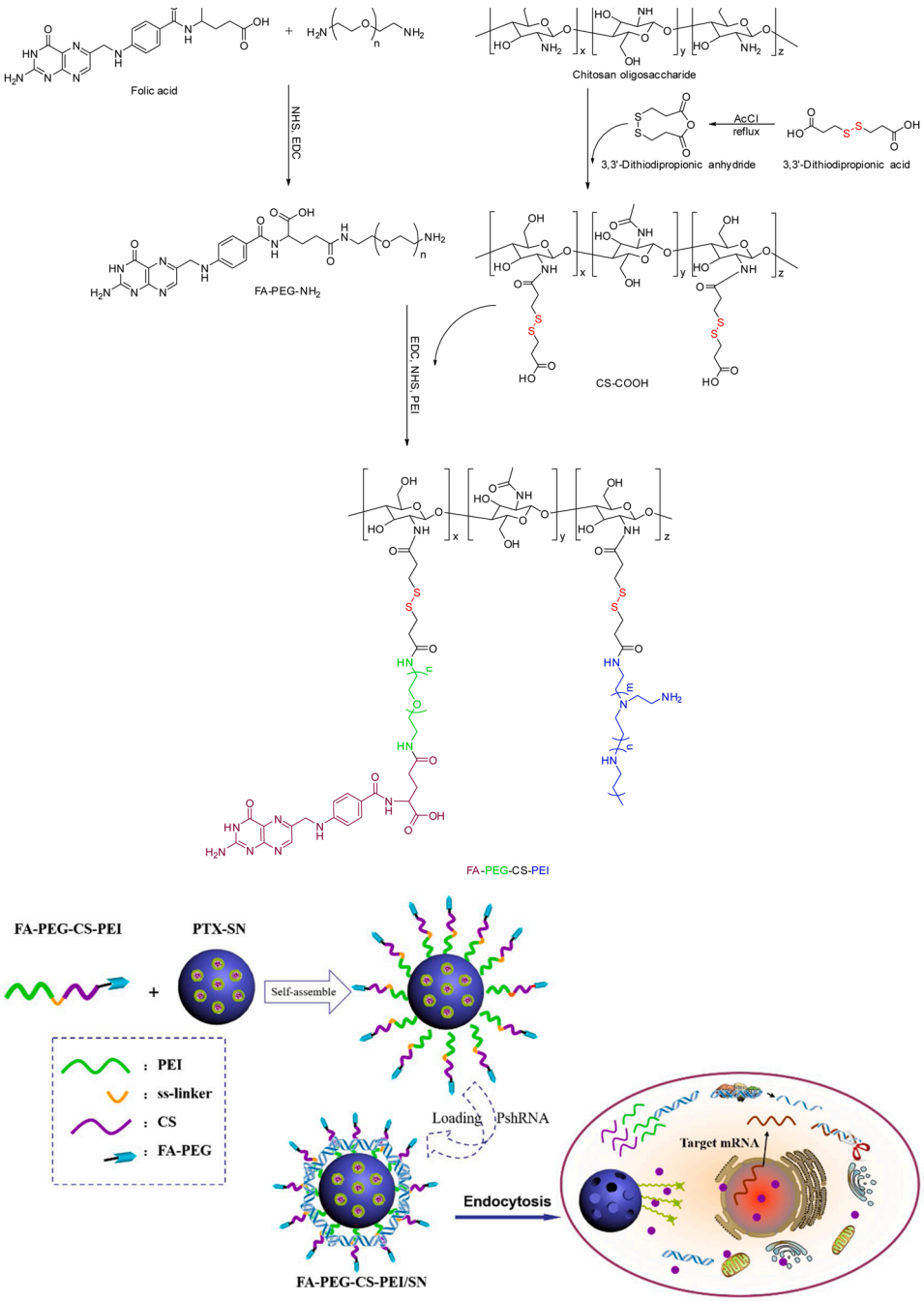

Scheme 1. Construction and mechanism illustration of folic acid-mediated chitosan oligosaccharide derivatives based nanohybrids for delivering Paclitaxel and P-shRNA.

2.2. Synthesis of FA-PEG-NH_2, CS-COOH and FA-PEG-CS-PEI polymer

2.2.1. Synthesis of FA-PEG-NH_2

25 mg of folic acid (FA) was dissolved in DMSO (5 mL), and then NHS (14 mg) and EDC (23 mg) were added. After stirring for 1 h, NH_2-PEG-NH_2 was added and the mixture was stirred for another 24 h. The product was purified by dialysis and then freeze-dried. The product was denoted as FA-PEG-NH_2.

2.2.2. Synthesis of CS-COOH

CS-COOH was synthesized according to a process that we previously reported (Jia et al., 2013). Briefly, 3,3'-dithiodipropionic acid (1 g) was dissolved into 5 mL of acetylchloride and refluxed for 2 h at 65 °C. After cooling down to ambient temperature, solvent was evaporated. Then, diethyl ether was used to precipitate the residue and washed repeatedly. The obtained product 3,3'-dithiodipropionic anhydride was dried overnight in a vacuum desiccator and applied directly in next step. CS powder (80 mg) was dissolved into 25 mL of distilled water following diluting with 10 mL of DMF. Then, 192 mg of 3,3'-dithiodipropionic anhydride was dissolved into DMF (10 mL) and added dropwise, and stirred for 8 h at ambient temperature. After purified by dialysis, the obtained product was collected by freeze-dried and denoted as CS-COOH.

2.2.3. Synthesis of FA-PEG-CS-PEI copolymer

The obtained CS-COOH was dissolved into distilled water (20 mL), and then NHS (115 mg) and EDC (191.7 mg) were added. After the reaction was stirred for 30 min at ambient temperature, FA-PEG-NH_2 (125

mg) was added and stirred for another 30 min. Subsequently, 10 ml of $PEI_{1.8k}$ solution was added to the mixture. After the reaction was stirred for 24 h, the obtained product was dialyzed, collected by freeze-dried, and denoted as FA-PEG-CS-PEI. The copolymer PEG-CS-PEI was constructed as control and synthesized as described in our previous study (Jia et al., 2013). ^{1}H NMR spectra were recorded to identify the structures of copolymers (on Varian inova, USA).

2.3. Synthesis of drug-loaded FA-PEG-CS-PEI/SN

The Paclitaxel (PTX) loaded silica nanoparticles (SN) with phosphoryl group (PTX-loaded SN-PO_4^{3-}) were prepared by the method of in situ self-assemble drug loading. The details are as follows. PTX (4 mg) and CTAB (100 mg) were dispersed in the distilled water and the mixture was stirred vigorously to obtain a clear solution at 75 °C. Subsequently, NH_4F was added dropwise to accelerate silica resources hydrolyzed and condensate. After 360 μL of TEOS was added, under a lucifugal condition, the reaction was stirred for 1 h. Then, 60 μL of methyl (3-trihydroxysilylpropoxy) phosphinate was added and reacted for another 30 min. Nanoparticles were collected through the method of centrifugation (10 min, 14000 rpm). Then, the obtained PTX-loaded SN-PO_4^{3-} were washed by ethanol and water to remove the unloaded CTAB and PTX. As for the blank SN-PO_4^{3-}, the process was the same described as above, except that the drug was not added and the CTAB was removed by refluxing in a mixture of 5 mL of hydrochloric acid (11.9 M) and 40 mL of ethanol.

The PTX-loaded SN-PO_4^{3-} or the blank SN-PO_4^{3-} was re-dispersed into water, and then the FA-PEG-CS-PEI copolymer was added dropwise following stir for 4 h. The uncombined copolymer was removed through centrifugation and the obtained hybrid nanoparticles was denoted as PTX-loaded FA-PEG-CS-PEI/SN or blank FA-PEG-CS-PEI/SN. PTX-loaded PEG-CS-PEI/SN was constructed as control.

2.4. DNA binding efficiency of FA-PEG-CS-PEI/SN

To assess DNA condensation ability of the FA-PEG-CS-PEI/SN or PEG-CS-PEI/SN, DNA binding efficiency was studied. Briefly, 0.1 μg of plasmid (6 μL) was blended with required amounts of nanoparticles to obtain 5, 10, 15, 20, 30, 40 and 50 N/P ratios, which were ratios of total nitrogen atoms (N) of nanoparticles to phosphate groups (P) of P-shRNA. Obtained complexes were simultaneously electrophoresed in 1% agarose gel, and naked P-shRNA was set as control. Gel electrophoresis was run in TAE buffer at room temperature for 20 min at 150 V. Bio-Rad Molecular Imager (ChemiDoc^{TM} XRS+) was applied to visualize DNA bands.

2.5. Dnase I protection Test

For excellent gene delivery, gene cargoes are able to be protected from enzymatic degradation by successful carriers. Dnase I protection test was applied to determine DNA protection efficiency of FA-PEG-CS-PEI/SN relative to positive control polymer PEI_{25k} at room temperature. Briefly, nanoparticle complexes were constructed as above described and then exposed to Dnase I (1U/μg P-shRNA). After incubating for 30 min, 8 μL of EDTA (pH 8.0, 0.5 M) was added to inactivate Dnase I. Subsequently, heparin (3 μL) was added and incubated for another 5 min. Agarose gel electrophoresis was performed to assess P-shRNA integrity as described above.

2.6. Construction and characterization of PTX and P-shRNA-loaded FA-PEG-CS-PEI/SN

2.6.1. Construction of PTX and P-shRNA-loaded FA-PEG-CS-PEI/SN

The PTX-loaded FA-PEG-CS-PEI/SN and P-shRNA was mixed in which the N/P ratio is 20, and incubated for 30 min at room temperature to obtained the co-loaded PTX and P-shRNA FA-PEG-CS-PEI/SN.

2.6.2. Particle size, morphology measurement and ζ-potential

ζ-potential and Particle size were measured by nanoparticle sizing measurement (Beckman Coulter, Delsa nano). Transmission electron microscope (JEM-1011, JEOL, Japan) was applied to observe morphologies of nanoparticles. Each sample was properly diluted to test with a suitable concentration, and all formulations was determined in triplicate.

2.6.3. Drug loading determination

Drug loading content was determined by detecting PTX in the supernatant after drugs thoroughly releasing from nanoparticles. The HPLC system was as below: Agilent 1100 series (Agilent), determination wavelength at 227 nm, Phenomenex-ODS column (5 mm, 150 mm × 4.60 mm), mobile phase of double-distilled water/acetonitrile (55/45, v/v) and 1.0 mL/min flow rate. Drug loading content was calculated as following equation:

$$\text{Drug loading content } (\%) = \frac{\text{Mass of drugs in nanoparticles}}{\text{Initial mass of nanoparticles}} \times 100\%$$

2.7. The Redox-responsive Destabilization and In vitro release of P-shRNA

The stability of co-loaded PTX and P-shRNA FA-PEG-CS-PEI/SN in response to 10 mM GSH was determined. In brief, 10 mM GSH solution was established to simulate intracellular redox conditions microenvironment and hybrid nanoparticles were added. Particle sizes of hybrid nanoparticles in suspensions were monitored at 0 h, 0.5 h, 1 h, 2 h, 4 h, 6 h, 8 h and 12 h, respectively. The colloidal stability of co-loaded PTX and P-shRNA FA-PEG-CS-PEI/SN in 150 mM NaCl was also studied as control.

To determine whether our reducible copolymers on the surface of nanoparticles were adequate to facilitate release of P-shRNA in 10 mM GSH solution, agarose gel electrophoresis was performed to assess amounts of released P-shRNA in the presence of heparin. Co-loaded PTX and P-shRNA FA-PEG-CS-PEI/SN were incubated in 10 mM GSH for 2 h and heparin (1 μL) was added. Other experimental conditions were consistent as described above.

2.8. In vitro drug release assay

The drugs release from co-loaded PTX and P-shRNA FA-PEG-CS-PEI/SN was investigated by the dialysis method. The "sink condition" was established by adding tween 80 into release mediums, which were acetic buffer solutions (pH 5.0, ABS) and phosphate buffer solutions (pH 7.4, 7.0, 6.5, PBS) containing Tween 80 (0.5% (w/v)) to simulate tumor and normal environments. Briefly, 2 mL of hybrid nanoparticles resuspension (loading 0.4 mg of drugs) was thrown into pre-swelled dialysis bags (MWCO = 8000–12000 Da), and subsequently, sealed dialysis bags were immersed into release medium at 37 °C. These release mediums were shaken in a light-sealed condition at the speed of 100 rpm. At different time intervals, samples of 1 mL were withdrawn and equal volumes of fresh release medium was immediately re-added. The concentration of PTX in samples was measured by the HPLC method as described above.

2.9. Evaluation of cytotoxicity of blank FA-PEG-CS-PEI/SN

Cytotoxicity of blank PEG-CS-PEI/SN and FA-PEG-CS-PEI/SN was measured using MTT assay in MCF-7/ADR. MCF-7/ADR cells were seeded at the density of 8000 cells/ 100 μL/well in 96-well plates. After 24 h incubation, blank nanoparticles were added at different particle concentrations. After incubated for 72 h, 20 μL of MTT was added to each well and incubated for another 4 h, and subsequently the medium was removed. Developed formazan crystals were dissolved by adding 200 μL of DMSO and the absorbance was measured at 570 nm using Bio-Rad680 microplate reader.

2.10. In vitro intracellular uptake of FA-PEG-CS-PEI/SN

Intracellular uptake and distribution of FA-PEG-CS-PEI/SN were investigated via fluorescent microscopy. To label nanoparticles, FITC was applied as the fluorescence probe. In brief, 4 mg of FITC dissolved in 2 mL of absolute ethanol and added dropwise into the FA-PEG-CS-PEI/SN dispersion with stirring for 12 h. FITC-labeled nanoparticles were subsequently harvested via centrifugation for 10 min at 14000 rpm. The obtained FITC-nanoparticles were dispersed into RPMI1640 medium (free folate) with a concentration of 10 μg/mL. When the growth density of MCF-7/ADR cells is at 60-70%, 1 mL of nanoparticle suspensions was added. After incubation for 1 h and 4 h, the medium was removed and cells were washed to remove residual nanoparticles by phosphate buffer saline. Then, the nucleus was stained by Hoechst 33342. Samples were observed via fluorescent microscopy.

The competitive binding test of free folic acid was also carried out to investigate roles of folate receptor in endocytosis of hybrid nanoparticles. MCF-7/ADR cells were firstly treated with 1 mM folic acid and then incubated with hybrid nanoparticles for 4 h. The intracellular uptake rate was detected through flow cytometry.

2.11. RT-PCR

Untreated and nanoparticles-treated cells were dealt with TRIzol reagent (Invitrogen) to extract total RNA. According to the manufacturer's instruction, cDNAs were synthesized by using the First Strand cDNA Synthesis Kit (Fermentas). The resulting cDNA was amplified by PCR using Taq DNA polymerase kit. PCR was conducted in a 50 μ L of reaction mixture according to the manufacturer's instruction, and cycling parameters included initial denaturation at 94 °C for 5 min, followed by 30 amplification cycles of 94 °C for 30 s, 58 °C for 30 s, and 72 °C for 1 min, and a final extension for 10 min at 72 °C. MDR1 forward and reverse primers were 5′-GGGAGCTTAACACCCGACTTA-3′ and 5′-GCCAAAATCACAAGGGTTAGCTT-3′, respectively. The GAPDH primer was used as internal control, and forward and reverse primers were 5′-CAAGGTCATCCATGACAACTTTG-3′ and 5′-GTCCACCACCCTGTTGCTGTAG-3′, respectively. Amplified products were separated on 1% agarose gels containing ethidium bromide and observed via Bio-Rad Molecular Imager (ChemiDocTM).

2.12. Western blot

The P-gp silencing efficiency of different P-shRNA and drug-loaded nanoparticles was assessed by the method of Western blotting. Briefly, cells were seeded and treated with different formulations. Subsequently cells were harvested and lysed in the lysis buffer (the lysis buffer consists of 5 mM tris, 15 mM NaCl, 0.1 mM EDTA, 0.1 mM EGTA, 5 mM sodium pyrophosphate, 50 mM NaF, 1 mM Na_3O_4, 1 mM β-glycerolphosphate, 5 μg/ml leupeptin, 1% Triton x-100 and 1 mM PMSF). The protein concentration was determined through the BCA assay. The protein sample was mixed with loading buffer, separated using 10% sodium dodecyl sulfate polyacrylamide gel electrophoresis and transferred onto polyvinylidene difluoride (PVDA) membranes. After immersed in blocking buffer, the membrane was incubated with primary antibody at 4 °C overnight and then incubated with secondary antibody at 37 °C for 1 h. The bands were finally visualized using enhanced chemiluminescence. β-actin was used as internal control.

2.13. Cell apoptosis

Cell apoptosis rate was analyzed by flow cytometry. MCF-7/ADR cells were treated with co-loaded PTX and P-shRNA FA-PEG-CS-PEI/SN at the PTX concentration of 20 nM, 40 nM and 80 nM, respectively. As a control, MCF-7/ADR cells were also exposed to co-loaded PTX and P-shRNA PEG-CS-PEI/SN with the PTX concentration of 20 nM, 40 nM, 80 nM, and free PTX at the concentration of 80 nM, respectively. After treating for 48 h, MCF-7/ADR cells were harvested and 400 μL of binding buffer was added. Subsequently, 5 μL of PI and 5 μL of Annexin V-FITC were added and incubated for 15 min at 25 °C in the dark. Samples were assessed using flow cytometer.

2.14. In vitro anti-tumor studies

MCF-7/ADR cells were seeded at the density of 8000 cells/ 100 μL/ well in 96-well plates. After 24 h incubation, blank nanoparticles were added at different particle concentrations. After incubated for 72 h, 20 μL of MTT was added to each well and incubated for another 4 h, and subsequently the medium was removed. Developed formazan crystals were dissolved by adding 200 μL of DMSO and the absorbance was measured at 570 nm using Bio-Rad680 microplate reader.

Antitumor activities in MCF-7 and MCF-7/ADR cells were determined by the MTT assay. Briefly, MCF-7/ADR and MCF-7 cells were seeded in 96-well plates, respectively. After 24 h incubation, designated wells were exposed to different concentrations of nanoparticles or free drugs. After treated for 72 h, 20 μL of MTT were added to each well and incubated for another 4 h, and subsequently the medium was removed. Developed formazan crystals were dissolved by adding 200 μL of DMSO and the absorbance was measured at 570 nm. Cell inhibitory rate was calculated as follows:

Cell inhibitory rate $=(1\text{-}Abs570_{\text{treated cells}} / Abs570_{\text{control cells}})\times 100\%$

IC_{50} is defined as the drug concentration required inhibiting cell growth by 50% compared with untreated controls.

3. Results and Discussions

3.1. Synthesis and Characteristics of FA-PEG-CS-PEI

In this study, folic acid (FA) was grafted to the polymer to improve effectively targeting to multidrug-resistant breast cells. In brief, folic acid was firstly activated by NHS ester, and NH_2-PEG-NH_2 was added into the reaction to obtained FA-PEG-NH_2. Meanwhile, 3,3'-dithiodipropionic acid was dehydrated to form anhydride to react with the amino groups in CS for obtaining CS-COOH. Then the CS-COOH was reacted with NHS ester, and FA-PEG-NH_2 was added. After reaction for 0.5 h, $PEI_{1.8k}$ solution was added into the mixture for reacting another 24 h to obtain the final product FA-PEG-CS-PEI. The process was illustrated as Scheme 1. PEG-CS-PEI was synthesized as control. The structure confirmation of these polymers was resorted to ^{1}H NMR spectra. As can be seen from Fig. 1, the characteristic peaks at 2.39–2.44 and 2.7–2.74 ppm were the signals of –CH_2CH_2S–, indicating 3,3'-dithiodipropionic acid grafted to the CS chain. Successful synthesis of FA-PEG-CS-PEI was confirmed by the characteristic peaks of –CH_2CH_2O– showed at 3.4–3.5 ppm, –$NHCH_2CH_2$– appeared at 2.5–3.0 ppm, aromatic nucleus of folic acid exhibited at 6.5–8.0 ppm and newly formed –CONH– discovered at 8.2–8.6 ppm implying PEG, PEI and folic acid were grafted to CS-COOH, respectively. As for PEG-CS-PEI, the characteristic peaks of PEG and PEI were all discovered, except folic acid. A buffer solution (0.2 M sodium acetate: 0.2 M acetic acid = 47 : 58) was applied as eluent at flow rate of 1 mL min^{-1}. The molecular weight of FA-PEG-CS-PEI copolymer was 24.1 kDa (M_w) measured by GPC with a PDI of 1.27.

Folic acid can specifically and strongly adhere to folate receptors which are overexpressed on the surface of breast cancer cells to mediate nanoparticles endocytosis (Xu, Bai, Zhang, & Yang, 2017). Thus, it is important for the content of folic acid in the polymers. The content of folic acid in FA-PEG-CS-PEI could be determined by UV Spectrophotometry. According to the regression equation (A = 0.0793 C-0.0038 (r = 0.9999)), the content of folic acid in FA-PEG-CS-PEI is 7.68%.

3.2. DNA binding efficiency and Dnase I protection assay

To investigate DNA loaded ability of FA-PEG-CS-PEI/SN or PEG-CS-

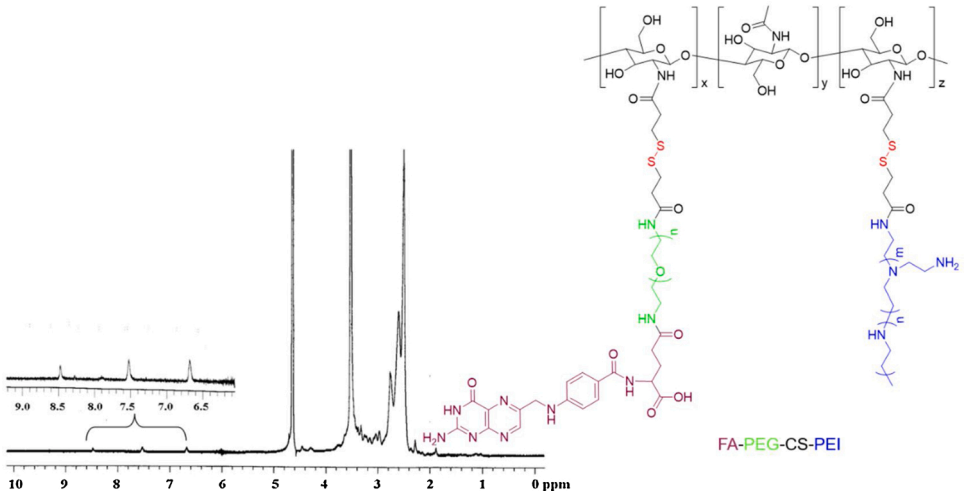

Fig. 1. The ^{1}H NMR spectra of FA-PEG-CS-PEI.

PEI/SN, DNA binding assay was performed. FA-PEG-CS-PEI/SN was the hybrid nanoparticles consisting of organic and inorganic materials. The cationic polymers on the surface of the nanoparticle provided a large number of positive charges which could be combined with negatively charged P-shRNA, so as to achieve codelivery of drugs and P-shRNA. We evaluated the ability of our fabricated hybrid nanoparticles to complex P-shRNA using agarose gel electrophoresis. It can be seen from Fig. 2(A) that the N/P ratio≥10:1 implied PEG-CS-PEI/SN effectively binding to P-shRNA. Compared with PEG-CS-PEI/SN, the binding ability of FA-PEG-CS-PEI/SN was slightly reduced (Fig. 2(B)). It was probably attributed to graft folic acid on the polymers to shield some of the positive charge. When the N/P ratio was equal to or greater than 15:1, the nanoparticles could be effectively combined with P-shRNA. It was deduced that low molecular weight $PEI_{1.8K}$ was effectively grafted based on CS as the backbone of carrier and our constructed copolymers on the surface of hybrid nanoparticles exhibited superior P-shRNA binding capacity.

Dnase I protection test was applied to evaluate whether FA-PEG-CS-PEI/SN could effectively protect P-shRNA from degradation before entering into cancer cells. As a positive control, the PEI 25k-P-shRNA complex was also treated with DNase I. As shown in Fig. 2(C, D), the naked P-shRNA (φ) was completely degraded after incubation with DNase I for 30 min. When P-shRNA was loaded with PEG-CS-PEI/SN, its ability to resist DNase I was significantly improved. When the N/P ratio was 15:1 or more, PEG-CS-PEI/SN could effectively protect P-shRNA. As for FA-PEG-CS-PEI/SN, the N/P ratio≥20:1 could provide effective protection for P-shRNA. These findings suggest that P-shRNA condensed onto our fabricated nanoparticles could be effectively protected.

3.3. Construction and characterization of codelivery of PTX and P-shRNA FA-PEG-CS-PEI/SN

To co-deliver PTX and P-shRNA, the drugs PTX were solubilized into the CTAB micelles in silica nanoparticles via in situ self-assembly method and the P-shRNA was complexed with the polymers which was coated on the surface of PTX-loaded SN. The morphologies of PEG-CS-PEI/SN, FA-PEG-CS-PEI/SN and SN were observed by TEM. As illustrated in Fig. 3, all nanoparticles had good dispersion and were spherical like. In addition, compared with the transmission electron micrograph of MSN (Fig. 3C), the profiles of PEG-CS-PEI/SN and FA-PEG-CS-PEI/SN (Fig. 3A, B) were fuzzy and their boundaries were not clear, which owed to the surface of the nanoparticles coated by co-polymers. Fig. 3(D–F) exhibited the particle size distribution of nano-particles, and the average particle sizes of PEG-CS-PEI/SN, FA-PEG-CS-PEI/SN and SN are 143.2, 138.7 and 92.4 nm, respectively with narrow particle size distribution. It was observed that the particle size of SN increased after being coated by copolymers. The charge on the surface of nanoparticles was measured by the zeta potential. We first measured the

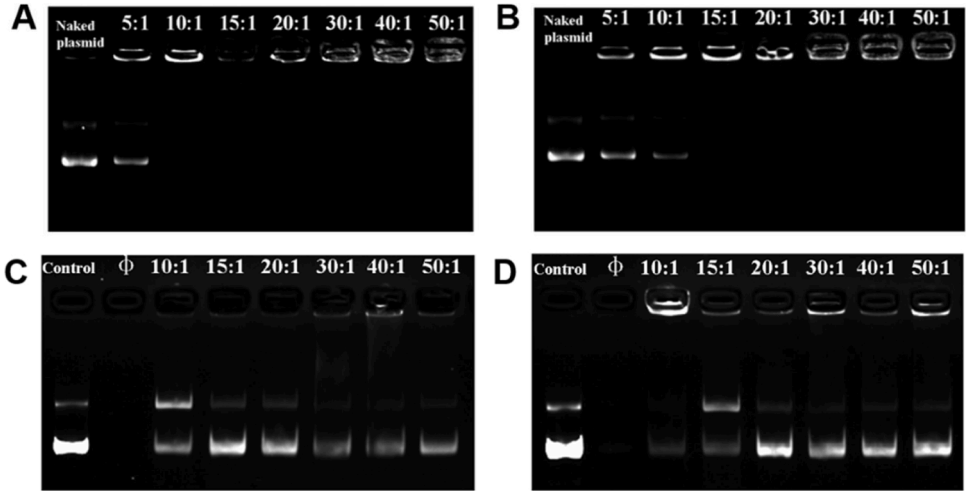

Fig. 2. Agarose gel electrophoresis of hybrid nanoparticles prepared at different N/P ratio: (A) PEG-CS-PEI/SN; (B) FA-PEG-CS-PEI/SN; hybrid nanoparticles protect P-shRNA from enzymatic degradation at different N/P ratios: (C) PEG-CS-PEI/SN; (D) FA-PEG-CS-PEI/SN.

Table 1
Characterization parameters of nanoparticles

Nanoparticles	Particle size (nm)	Polydispersity index	Zeta potential (mV)	Drug loading (%)
MSN	92.4 ± 8.2	0.107 ± 0.005	−38.7 ± 2.36	8.35 ± 0.67
PEG-CS-PEI/SN (N/P = 20)	143.2 ± 11.3	0.112 ± 0.003	+11.42 ± 1.45	7.82 ± 0.34
FA-PEG-CS-PEI/SN (N/P = 20)	138.7 ± 10.7	0.116 ± 0.004	+9.87 ± 1.32	7.43 ± 0.29

zeta potential of SN which had negative charge owing to PO_4^{3-} on the surface of nanoparticles, and the average zeta potential was -38.7 mV. After the SN recombining with PEG-CS-PEI or FA-PEG-CS-PEI, the zeta potential of obtained hybrid nanoparticles was measured as positive, and the average zeta potential was 33.1 and 30.7 mV, respectively, indicating the cationic polymers neutralized the negative charge of PO_4^{3-}-SN and left a large number of positive charges existed on the surface of hybrid nanoparticles. These positive charges could be applied to further condense P-shRNA via electrostatic interaction. According to the results of DNA binding efficiency and Dnase I protection assay, we constructed PTX and P-shRNA co-loaded hybrid nanoparticles with N/P ratio of 20:1 for further investigation, and their zeta potential and drug loading are shown in Table 1.

3.4. In vitro release of P-shRNA and Redox-responsive Destabilization

In order to evaluate whether FA-PEG-CS-PEI/SN could effectively release P-shRNA in the intracellular reductive microenvironment, 10 mm GSH solution was used to simulate the reducing microenvironment and gel electrophoresis was applied to investigate the response of these hybrid nanoparticles to GSH. The results are exhibited in Fig. 4(A, B). In the absence of GSH, although the complex was incubated with heparin for a certain period of time, it did not release P-shRNA. Nevertheless, P-shRNA could be effectively released from hybrid nanoparticles in 10 mM GSH condition. Therefore, it was deduced that disulfide linkages in co-polymers on the hybrid nanoparticles were relatively stable in the extracellular environment, but once nanoparticles endocytosis by cancer cells, disulfide linkages were cleaved to form CS and $PEI_{1.8K}$ fragments under the reducing intracellular environment, which could not compress the plasmid effectively owing to the low charge density and P-shRNA could be effectively released.

The change of the particle size of FA-PEG-CS-PEI/SN in 10 mM GSH solution was also monitored to predict the stability of hybrid nanoparticles in cancer cells. As exhibited in Fig. 4(C), the particle size of FA-PEG-CS-PEI/SN in nonreducing environment (150 mM NaCl) was almost unchanged after 12 hours, showing good stability. However, with the increase of incubation time in 10 mM GSH solution, the particle size of nanoparticles increased first and then decreased. It could be explained that the disulfide bonds of the copolymer on the surface of nanoparticles gradually broke and the structure became loose with the action of GSH. Through dynamic light scattering detection, the particle size gradually increased and the maximum particle size was 185 nm at 6 h. Then the broken fragments such as PEG and $PEI_{1.8K}$ gradually separated from the nanoparticle surface and integrated into the dispersion medium, and hence the copolymer layer on the nanoparticle surface became thin. Then, the overall particle size of the nanoparticles decreased by dynamic light scattering detection, and the particle size was 154 nm at 12 h. The above results revealed that our fabricated hybrid nanoparticles possessed excellent GSH response characteristics, which could maintain good stability outside cancer cells to protect P-shRNA from enzyme degradation. Once into the cell, under the effect of GSH, the P-shRNA could be effectively released to silence the mRNA and knock down the expression of P-gp.

The stability of FA-PEG-CS-PEI/SN in PBS (pH 7.4) as well as RPMI1640 + 10% FBS for 7 days was investigated. As displayed in Fig. S1, the particle size of these nanohybrids remained almost unchanged in PBS for 7 days and only slight fluctuation in RPMI1640 + 10%FBS, which suggested that these nanohybrids were stable in physiological environments and could protect their cargos within circulation.

3.5. In vitro release of PTX from FA-PEG-CS-PEI/SN

It is well known that diseased tissues (inflammation, tumors and ischemia) possess the acidic environment. Besides, intracellular organelles, such as endosomes and lysosomes, exhibit more acidic pH values (6.8–4.5) (Cardone, Casavola, & Reshkin, 2005; Yuan, Peng, Lin, Wang, & Zhang, 2019). In this study, PTX released from hybrid nanoparticles in vitro were performed in various pH buffers (pH 5.0, 6.5, 7.0 and 7.4), as illustrated in Fig. 4(D). In the neutral solution, PTX was released slowly and the cumulative release rate of PTX was only 7.9% at 72 hours. When the release medium was weak acid, the release rate of the drug was obviously accelerated. In the release medium of pH 5.0, the cumulative release rate of PTX was 54.1% at 72 hours. The above results exhibited that FA-PEG-CS-PEI/SN exhibited excellent pH- pH-stimuli release, which may be relevant to CTAB micelles in the nanopore. CTAB micelles are stable in the neutral media, while cations in CTAB could swap with protons in the acidic environment, which make the micelles more easily destroyed (Huo, Margolese, Ciesla, Feng, Gier, Sieger, Leon, Petroff, Schüth, & Stucky, 1994). PTX was incorporated into CTAB micelles via

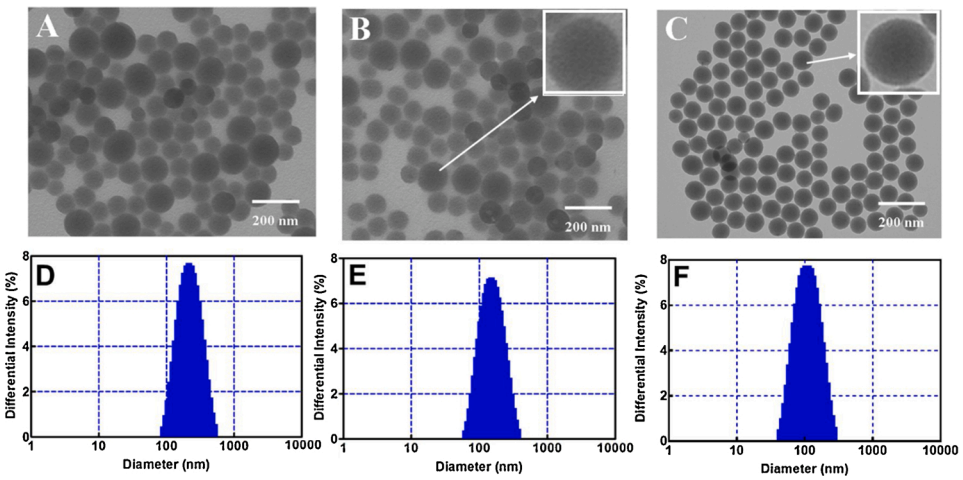

Fig. 3. The TEM images of(A)PEG-CS-PEI/SN,(B)FA-PEG-CS-PEI/SN,(C)SN; the particle size distributions of(D)PEG-CS-PEI/SN ; (E)FA-PEG-CS-PEI/SN ; (F)SN.

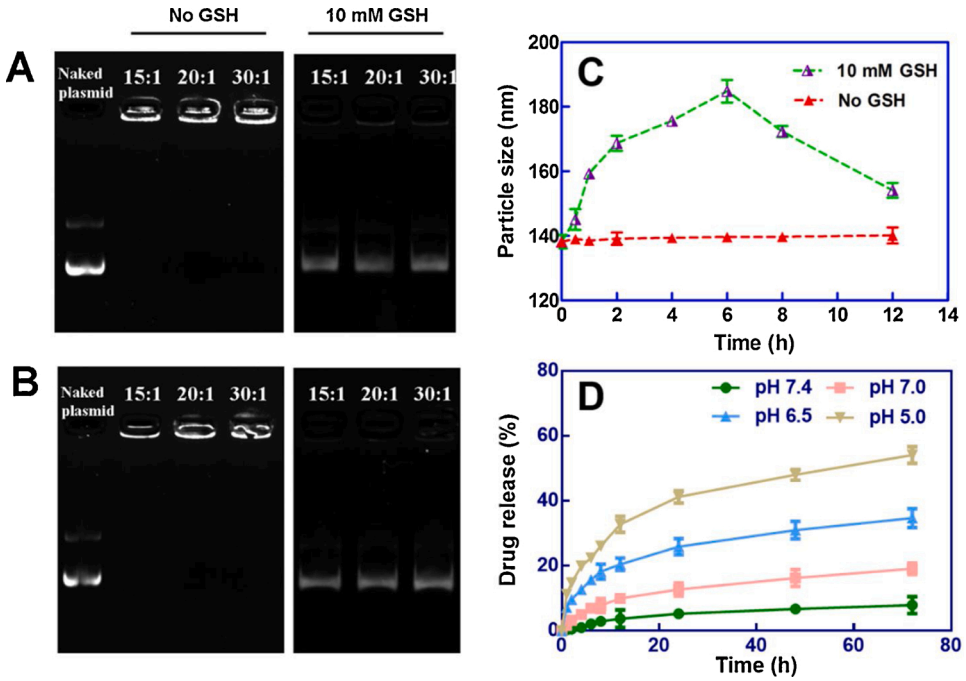

Fig. 4. Redox-induced release of P-shRNA from(A)PEG-CS-PEI/SN ; (B)FA-PEG-CS-PEI/SN; (C)the influence of GSH on particle size of polyplexes prepared form FA-PEG-CS-PEI/SN; (D)in vitro release profiles of PTX from FA-PEG-CS-PEI/SN at different pH values.

in situ self-assemble drug loading method in the FA-PEG-CS-PEI/SN. CTAB micelles containing drugs exhibit more stability in the neutral media, and either CTAB molecules or drugs are difficult to escape from nanopores of FA-PEG-CS-PEI/SN. However, in the sites of tumors or uptake by tumor cells, structures of micelles are disrupted, and drugs and CTAB molecules have more chances to be released from nanopores of hybrid nanoparticles. Therefore, CTAB is not only as the part of hybrid nanoparticles but also the pH-stimuli switch to control the release of drugs that led to FA-PEG-CS-PEI/SN possessed well pH-sensitive release drug behaviors.

To evaluate whether FA-PEG-CS-PEI/SN possessed redox-stimuli responsive drug release properties, nanohybrids were dispersed in the different release medium: pH 7.4 PBS with 10 mM GSH, pH 7.0 PBS with 10 mM GSH, pH 6.5 PBS with 10 mM GSH and pH 5.0 PBS with 10 mM GSH, respectively. As shown in Fig. S2, the cumulative release of PTX was further improved in presence of GSH at the same pH environment. The reasons are as follows. In presence of high concentration of GSH, the disulfide bonds of FA-PEG-CS-PEI/SN were broken, the broken fragments such as PEG and $PEI_{1.8K}$ gradually separated from the nanoparticle surface and hence the copolymer layer on the nanoparticle

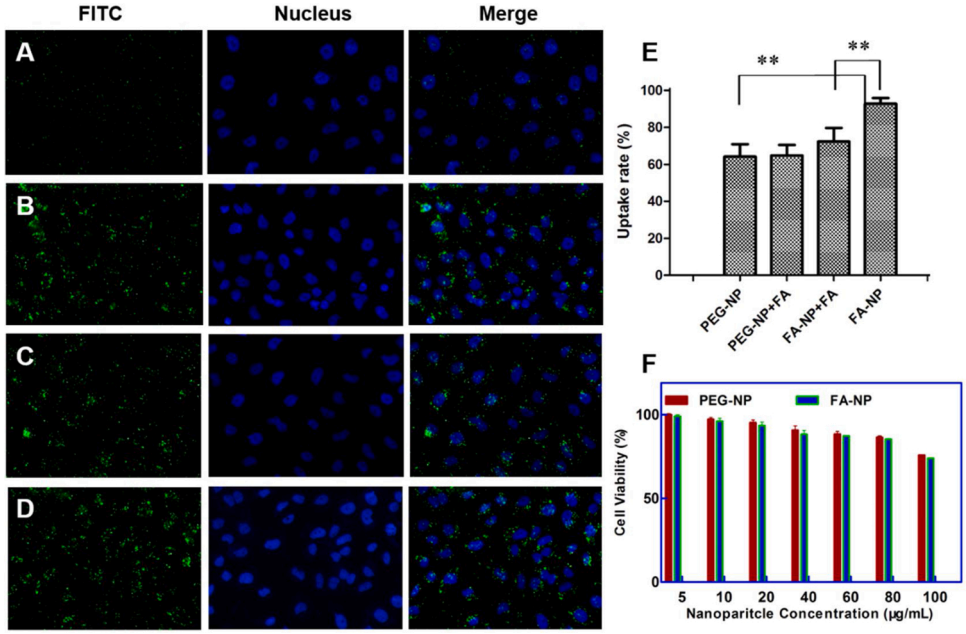

Fig. 5. Cell uptake of (A) FITC-PEG-CS-PEI/SN at 1 h; (B) FITC-PEG-CS-PEI/SN at 4 h; (C) FITC-FA-PEG-CS-PEI/SN at 1 h; (D) FITC-FA-PEG-CS-PEI/SN at 4 h; (E) Fluorescence intensity of cells analyzed by flow cytometric after treated with nanoparticles at 4 h; (F) Cell viabilities of blank nanoparticles in MCF-7/ADR cells (n = 3).

surface became thin, which allowed the fast release of PTX from the nanohybrids to the release medium. Although cumulative release of PTX could be improved in 10 mM GSH, the pH environment is the dominant factor in drug release of these nanohybrids.

3.6. Biocompatibility and uptake of hybrid nanoparticles

The cytotoxicity and intracellular uptake of FA-PEG-CS-PEI/SN and PEG-CS-PEI/SN were investigated in multidrug resistant cells MCF-7/ADR. The MTT assay used for evaluating blank hybrid nanoparticles cytotoxicity shows that as high as 80 μg/ml nanoparticles had no obvious toxicity to both PEG-CS-PEI/SN (PEG-NP) and FA-PEG-CS-PEI/SN (FA-NP) group, with cell viability higher than 85% after 72 h treatment (Fig. 5(F)). There was no significant difference in cytotoxicity between PEG-CS-PEI/SN and FA-PEG-CS-PEI/SN ($P > 0.05$). Therefore, the hybrid nanoparticles exhibited well biocompatibility.

Fluorescence microscopy was applied to observe the uptake of FITC-labeled hybrid nanoparticles. MCF-7/ADR cells were incubated with FITC labeled PEG-CS-PEI/SN and FA-PEG-CS-PEI/SN, and photographed at 1 h and 4 h, respectively. As shown in Fig. 5, slight fluorescence was observed in the PEG-CS-PEI/SN group (Fig. 5A) at 1 h, but the FA-PEG-CS-PEI/SN group (Fig. 5B) had obvious fluorescence uptake, indicating that grafting folic acid on the hybrid nanoparticles was conducive to the rapid uptake of the nanoparticles by cells. With the prolongation of incubation time (at 4 h), the green fluorescence of both hybrid nanoparticle groups increased significantly, while the uptake of targeted nanoparticles was the highest (Fig. 5D). In order to further investigate the role of folate receptor in the process of FA-PEG-CS-PEI/SN uptake by MCF-7/ADR cells, the competitive binding test of free folic acid was carried out. As shown in Fig. 5(E), when FA-PEG-CS-PEI/SN was incubated with cells for 4 hours, the fluorescence uptake rate was 93%. However, MCF-7/ADR cells were treated with 1 mM free folic acid first, the fluorescence uptake rate of the targeted nanoparticles group was significantly reduced to 65.8%, but there was no significant difference between PEG-CS-PEI/SN groups. The results revealed that the increased uptake of FA-PEG-CS-PEI/SN was probably due to the folate receptor mediated endocytosis.

3.7. RT-PCR and Western blot

The downregulation of P-gp using small RNA interference technology has been considered as a potential therapeutic option for reversing multidrug resistance in cancer cells (Lage & Hermann, 2006). In this test, the MDR1 gene silencing effect was determined by MDR1 mRNA levels using RT-PCR and amplified products were separated on agarose gels. MDR1 mRNA expression was firstly detected in resistant and sensitive cell lines without treatment. As shown in Fig. 6(A and B), MDR1 mRNA was overexpressed in the resistant cell line MCF-7/ADR, while MDR1 mRNA expression was almost not detected in the sensitive cell line MCF-7. After MCF-7/ADR cells were treated with hybrid nanoparticles, both PEG-CS-PEI/SN and FA-PEG-CS-PEI/SN group significantly interfered with MDR1 mRNA, among which the FA-PEG-CS-PEI/SN (at N/P = 30) induced a 78% decrease of MDR1 mRNA. We also assessed the efficiency of FA-PEG-CS-PEI/SN in inhibiting P-gp expression in the MCF-7/ADR cell lines by western blot. The results are exhibited in Fig. 6(C). P-gp was overexpressed in the resistant cell line MCF-7/ADR, but almost no P-gp was detected in the sensitive cell line implying MCF-7/ADR cells had serious drug resistance in this study. We investigated the effect of hybrids nanoparticles on the expression of P-gp in MCF-7/ADR cells and the results are consistent with RT-PCR. Namely, our synthesized nanoparticles could significantly inhibit the expression of P-gp and induced 33%, 49% and 63% decrease at PEG-CS-PEI/SN (N/P = 20:1), FA-PEG-CS-PEI/SN (N/P = 20:1) and FA-PEG-CS-PEI/SN (N/P = 30:1) group, respectively. Thus, the results indicated that the FA-PEG-CS-PEI/SN could effectively deliver P-shRNA into MCF-7/ADR cells, and showed high gene silencing efficiency at the targeted mRNAs to downregulate the expression of P-gp.

3.8. Cell apoptosis assay

To investigate apoptotic effects of our constructed nanoparticles quantitatively, flow cytometer was performed to determine percentages of cell apoptosis. As in Fig. 7, the mean percentage of early and late apoptosis of MCF-7/ADR cells treated with PTX solution at the concentration of 80 nM was 0.62%, suggesting that cells possessed drug resistance, and almost no apoptosis occurred. Compared with free PTX group, PEG-CS-PEI/SN formulations markedly increased the apoptosis rate and the average apoptosis rate was 21.99% at the PTX concentration of 80 nM, which was significantly higher than that of the PTX solution group ($P < 0.01$). As for the targeted formulations FA-PEG-CS-PEI/SN group, the apoptosis rate increased with the increase of drug concentration, and the average apoptosis rate was 30.26% and 48.06% at the drug concentration of 40 nM and 80 nM, respectively, which were significantly higher than that of PEG-CS-PEI/SN group ($P < 0.01$). It was deduced that the hybrid nanoparticles were additionally taken up though folic acid via endocytosis, and subsequently loaded P-shRNA released and inhibited the function of P-gp efflux pump to increase intracellular numbers of nanoparticles finally leading to cell apoptosis enhancement.

3.9. In vitro reversal MDR and antitumor activities

On the basis of the results above, FA-PEG-CS-PEI/SN was proved to possess an excellent capability for co-delivering P-shRNA and PTX. In

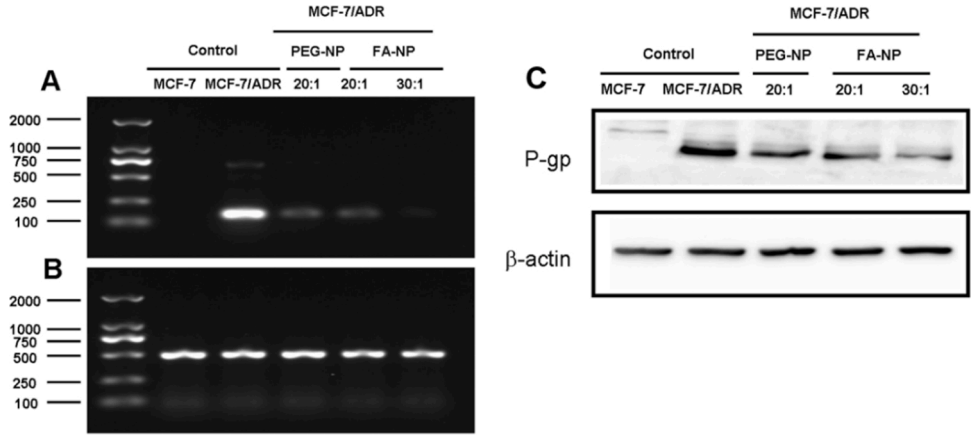

Fig. 6. Agarose gel electrophoresis of RT-PCR products: (A) MDR1; (B) GAPDH; (C) Western blot for P-gp.

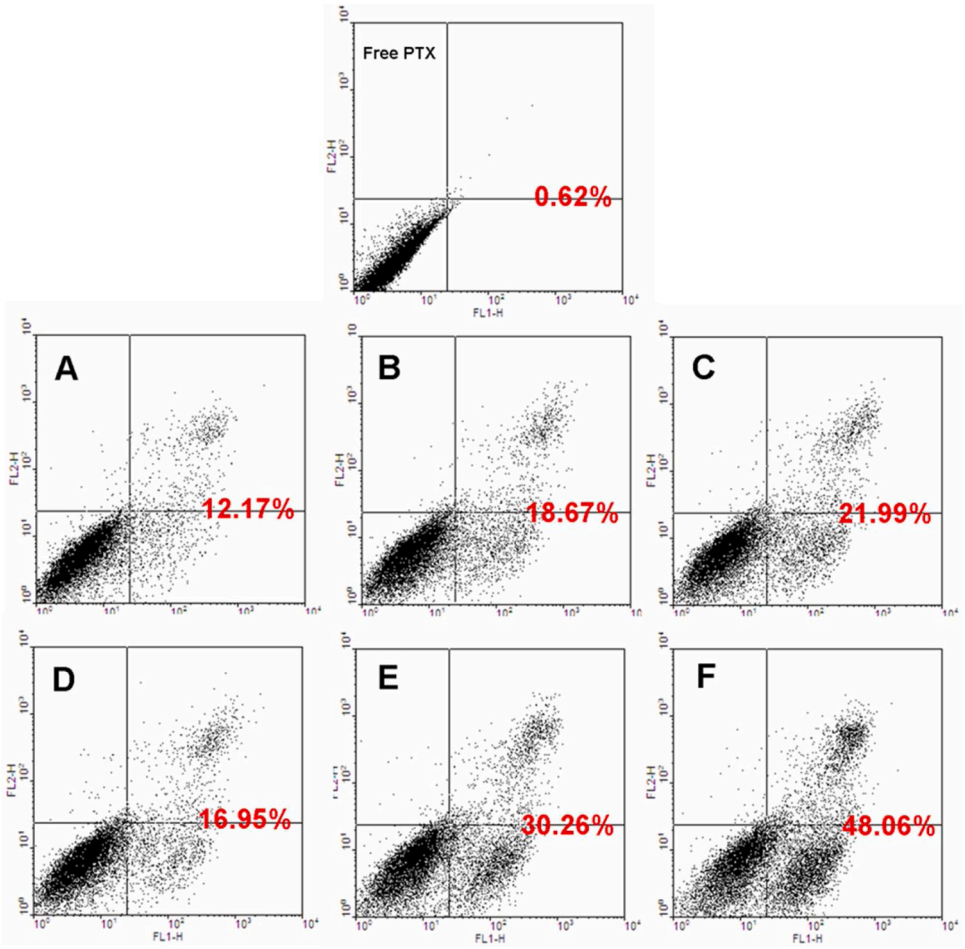

Fig. 7. Flow cytometry analysis of MCF-7/ADR cells after treatment with PEG-CS-PEI/SN with the PTX concentration of (A) 20 nM; (B) 40 nM; (C) 80 nM; and FA-PEG-CS-PEI/SN with the PTX concentration of (D) 20 nM; (E) 40 nM; (F) 80 nM; and free PTX with the concentration of 80 nM.

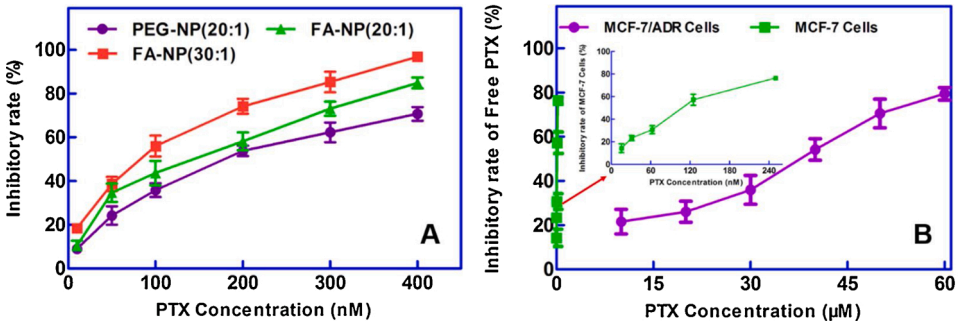

Fig. 8. In vitro antitumor activities of nanoparticles in MCF-7/ADR cells (A) and PTX solution in both kinds of cells (B).

this study, we investigated the reversal efficacy and antitumor activities of hybrid nanoparticles in MCF-7 cells and MCF-7/ADR cells. Before to study antitumor activities of these hybrid nanoparticles, the efficacy of free PTX on cytotoxicity of cells was tested. As shown in Fig. 8(B), free PTX led to significantly more cytotoxicity on MCF-7 than MCF-7/ADR cells. Compared to drug-sensitive MCF-7 cells (IC_{50} = 88.6 nM), MCF-7/ADR cells (IC_{50} = 3.89 mM) in this study were approximately 44-fold more resistant to drugs. Fig. 8(A) illustrates the growth inhibition curve of hybrid nanoparticles to MCF-7/ADR cells. It can be seen that the inhibition rate of two kinds of nanoparticles to drug-resistant cells is higher than that of PTX solution group. Compared with PEG-CS-PEI/SN group, two targeted preparations exhibited higher inhibitory effect on MCF-7/ADR cells.

Table 2
IC_{50} (mean ± S.D.) and resistance reversion index (RRI) of various agents against MCF-7 or MCF-7/ADR cells.

Sample	MCF-7/ADR cells	
	IC_{50} (nM)	RRI
Free PTX	$3.89 \times 10^3 \pm 230$	-
PEG-CS-PEI/SN (20:1)	153.1 ± 15.3	25.41
FA-PEG-CS-PEI/SN (20:1)	114.4 ± 11.6	34.00
FA-PEG-CS-PEI/SN (30:1)	76.9 ± 4.8	50.59

The reversal activity is expressed as the resistance reversion index (RRI) calculated according to the following equation: (RRI) = $IC_{50\ (free\ PTX)}$ / $IC_{50\ (PTX\ formulations)}$.

The IC_{50} values of different kinds of hybrid nanoparticles to MCF-7/ADR cells are depicted in Table 2, which were 153.1 nM, 114.4 nM and 76.9 nM for PEG-CS-PEI/SN (N/P = 20:1), FA-PEG-CS-PEI/SN (20:1) and FA-PEG-CS-PEI/SN (30:1), respectively. The IC_{50} values of two targeted nanoparticles are significantly lower than that of the common nanoparticle ($P < 0.05$). Such low IC_{50} of hybrid nanoparticles indicated high drug efficiencies against MCF-7/ADR cells, and meanwhile implied expected using low amounts of drugs and carriers. It was hinted that our hybrid nanoparticles were efficiently taken up by cells and released P-shRNA to knock down the expression of P-gp which would inhibit the efflux of nanoparticles and increase drug accumulation in cells. In addition, it was found that PTX resistance in MCF-7/ADR cells could be completely reversed by the FA-PEG-CS-PEI/SN (30:1) and resistance reversion index (RRI) was 50.59 (IC_{50} value of paclitaxel in sensitive cell lines is 88.6 ± 8.7 nm). All the in vitro antitumor studies indicated FA-PEG-CS-PEI/SN could efficiently co-deliver P-shRNA and PTX into breast cancer cells to exert synergistic antitumor activity.

4. Conclusion

In this work, we have successfully developed a folic acid mediated chitosan oligosaccharide-based disulfide-containing polyethylenimine copolymer-based silica nanohybrids for co-delivering P-shRNA and paclitaxel to overcoming multidrug resistance of breast cancer cells. The hybrid nanoparticles exhibited excellent redox-responsive P-shRNA release and pH-sensitive drug release behaviors to protect genes from degradation and prevent the premature loss of drugs before entering into cancer cells. Besides, folic acid ligands in the copolymer could selectively facilitate the internalization of hybrid nanoparticles for breast cancer cells through receptor-mediated endocytosis. Moreover, it was demonstrated that the FA-PEG-CS-PEI/SN could effectively deliver P-shRNA into MCF-7/ADR cells, and showed high gene silencing efficiency at the targeted mRNAs to downregulate the expression of P-gp for increase of intracellular drug concentration. In the antitumor activity study, the proliferation of MCF-7/ADR cells was significantly inhibited by PTX and P-shRNA co-loaded hybrid nanoparticles and the resistance to paclitaxel was completely reversed. Hence, our constructed hybrid nanoparticles have a great potential as a drug delivery platform for drugs and genes combination therapy in overcoming cancer multidrug resistance.

Declaration of Competing Interest

The authors report no declarations of interest.

CRediT authorship contribution statement

Lejiao Jia: Conceptualization, Methodology, Writing - original draft. **Zhenyu Li:** Methodology, Data curation. **Dandan Zheng:** Visualization, Investigation. **Zhiying Li:** Validation. **Zhongxi Zhao:** Supervision, Writing - review & editing.

Acknowledgments

This work was financially supported by the National Natural Science Foundation of China (No. 81402868, 81502921), Major Project of Science and Technology of Shandong Province (Grant #2018CXGC1411) and Distinguished Middle-Aged and Young Scientist Encourage and Reward Foundation of Shandong Province (No. BS2014YY007).

Appendix A. Supplementary data

Supplementary material related to this article can be found, in the online version, at doi:https://doi.org/10.1016/j.carbpol.2020.117008.

References

Alavi, M., & Hamidi, M. (2019). Passive and active targeting in cancer therapy by liposomes and lipid nanoparticles. *Drug metabolism and personalized therapy*, 34.
Antony, A. C. (1996). Folate Receptors. *Annual Review of Nutrition, 16*, 501–521.
Aquib, M., Farooq, M. A., Banerjee, P., Akhtar, F., Filli, M. S., Boakye-Yiadom, K. O., et al. (2019). Targeted and stimuli-responsive mesoporous silica nanoparticles for drug delivery and theranostic use. *J Biomed Mater Res A, 107*, 2643–2666.
Baguley, B. C. (2010). Multiple Drug Resistance Mechanisms in Cancer. *Molecular Biotechnology, 46*, 308–316.
Bartlett, D. W., & Davis, M. E. (2007). Effect of siRNA nuclease stability on the in vitro and in vivo kinetics of siRNA-mediated gene silencing. *Biotechnology & Bioengineering, 97*, 909–921.
Bukowski, K., Kciuk, M., & Kontek, R. (2020). Mechanisms of Multidrug Resistance in Cancer Chemotherapy. *Int J Mol Sci, 21*, 3233.
Cardone, R. A., Casavola, V., & Reshkin, S. J. (2005). The role of disturbed pH dynamics and the Na+/H+ exchanger in metastasis. *Nature Reviews Cancer, 5*, 786–795.
Chen, F., Zhao, E. R., Hableel, G., Hu, T., Kim, T., Li, J., et al. (2019). Increasing the Efficacy of Stem Cell Therapy via Triple-Function Inorganic Nanoparticles. *ACS nano, 13*, 6605–6617.
Cheng, R., Feng, F., Meng, F., Deng, C., Feijen, J., & Zhong, Z. (2011). Glutathione-responsive nano-vehicles as a promising platform for targeted intracellular drug and gene delivery. *Journal of controlled release : official journal of the Controlled Release Society, 152*, 2–12.
Curiel, T. J. (2012). Immunotherapy: a useful strategy to help combat multidrug resistance. *Drug Resist Updat, 15*, 106–113.
Gottesman, M. M., Fojo, T., & Bates, S. E. (2002). Multidrug resistance in cancer: Role of ATP-dependent transporters. *Nature Reviews Cancer, 2*, 48–58.
Guerry, A., Cottaz, S., Fleury, E., Bernard, J., & Halila, S. (2014). Redox-stimuli responsive micelles from DOX-encapsulating polycaprolactone-g-chitosan oligosaccharide. *Carbohydr Polym, 112*, 746–752.
Holohan, C., Van Schaeybroeck, S., Longley, D. B., & Johnston, P. G. (2013). Cancer drug resistance: an evolving paradigm. *Nature Reviews Cancer, 13*, 714–726.
Huang, H., Yu, H., Tang, G., Wang, Q., & Li, J. (2010). Low molecular weight polyethylenimine cross-linked by 2-hydroxypropyl-gamma-cyclodextrin coupled to peptide targeting HER2 as a gene delivery vector. *Biomaterials, 31*, 1830–1838.
Huo, Q., Margolese, D. I., Ciesla, U., Feng, P., Gier, T. E., Sieger, P., et al. (1994). Generalized synthesis of periodic surfactant/inorganic composite materials. *Nature, 368*, 317–321.
Jörg, H., Baehr, C., Kiermayer, S., Zeuzem, S., & Piiper, A. (2006). Inhibition of RNAse A family enzymes prevents degradation and loss of silencing activity of siRNAs in serum. *Biochemical Pharmacology, 71*, 702–710.
Jia, L., Li, Z., Zhang, D., Zhang, Q., Shen, J., Guo, H., et al. (2013). Redox-responsive catiomer based on PEG-ss-chitosan oligosaccharide-ss-polyethylenimine copolymer for effective gene delivery. *Polymer Chemistry, 4*, 156–165.
Johnstone, R. W., Ruefli, A. A., & Lowe, S. W. (2002). Apoptosis: A Link between Cancer Genetics and Chemotherapy. *Cell, 108*, 153–164.
Kresge, C. T., Leonowicz, M. E., Roth, W. J., Vartuli, J. C., & Beck, J. S. (1992). Ordered mesoporous molecular sieves synthesized by a liquid-crystal template mechanism. *Nature, 359*, 710–712.
Lage, & Hermann. (2006). MDR1/P-Glycoprotein (ABCB1) as Target for RNA Interference-Mediated Reversal of Multidrug Resistance. *Current Drug Targets, 7*, 813–821.
Lai, Q. Y., He, Y. Z., Peng, X. W., Zhou, X., Liang, D., & Wang, L. (2019). Histone deacetylase 1 induced by neddylation inhibition contributes to drug resistance in acute myelogenous leukemia. *Cell communication and signaling : CCS, 17*, 86.
Li, Q. L., Wang, D., Cui, Y., Fan, Z., Ren, L., Li, D., et al. (2018). AIEgen-Functionalized Mesoporous Silica Gated by Cyclodextrin-Modified CuS for Cell Imaging and Chemo-Photothermal Cancer Therapy. *ACS applied materials & interfaces, 10*, 12155–12163.
Li, R., Lin, Z., Zhang, Q., Zhang, Y., Liu, Y., Lyu, Y., et al. (2020). In SituInjectable and -Formable Thiolated Chitosan-Coated Liposomal Hydrogels as Curcumin Carriers for Prevention of Breast Cancer Recurrence. *ACS applied materials & interfaces, 12*, 17936–17948.
Liu, M., Anderson, R. C., Lan, X., Conti, P. S., & Chen, K. (2020). Recent advances in the development of nanoparticles for multimodality imaging and therapy of cancer. *Med Res Rev, 40*, 909–930.
Longley, D., & Johnston, P. (1990). Molecular mechanisms of drug resistance. *The Journal of pathology, 272*, 281–295.
Lungwitz, U., Breunig, M., Blunk, T., & Gopferich, A. (2005). Polyethylenimine-based non-viral gene delivery systems. *European journal of pharmaceutics and biopharmaceutics, 60*, 247–266.
Luo, T., Han, J., Zhao, F., Pan, X., Tian, B., Ding, X., et al. (2019). Redox-sensitive micelles based on retinoic acid modified chitosan conjugate for intracellular drug delivery and smart drug release in cancer therapy. *Carbohydr Polym, 215*, 8–19.
Madheswaran, T., Kandasamy, M., Bose, R. J., & Karuppagounder, V. (2019). Current potential and challenges in the advances of liquid crystalline nanoparticles as drug delivery systems. *Drug discovery today, 24*, 1405–1412.
Mahon, F. X., Belloc, F., Lagarde, V., Chollet, C., Moreau-Gaudry, F., Reiffers, J., et al. (2003). MDR1 gene overexpression confers resistance to imatinib mesylate in leukemia cell line models. *Blood, 101*, 2368–2373.
Miao, J., Yang, X. Q., Gao, Z., Li, Q., Meng, T. T., Wu, J. Y., et al. (2019). Redox-responsive chitosan oligosaccharide-SS-Octadecylamine polymeric carrier for efficient anti-Hepatitis B Virus gene therapy. *Carbohydr Polym, 212*, 215–221.
Mizutani, T., Masuda, M., Nakai, E., Furumiya, K., Togawa, H., Nakamura, Y., et al. (2008). Genuine Functions of P-Glycoprotein (ABCB1). *Current Drug Metabolism, 9*, 167–174.

Mu, Y., Wu, G., Su, C., Dong, Y., Zhang, K., Li, J., et al. (2019). pH-sensitive amphiphilic chitosan-quercetin conjugate for intracellular delivery of doxorubicin enhancement. *Carbohydr Polym, 223*, Article 115072.

Musalli, A. H., Talukdar, P. D., Roy, P., Kumar, P., & Wong, T. W. (2020). Folate-induced nanostructural changes of oligochitosan nanoparticles and their fate of cellular internalization by melanoma. *Carbohydr Polym, 244*, Article 116488.

Nie, Y., Gunther, M., Gu, Z., & Wagner, E. (2011). Pyridylhydrazone-based PEGylation for pH-reversible lipopolyplex shielding. *Biomaterials, 32*, 858–869.

Nomoto, T., Matsumoto, Y., Miyata, K., Oba, M., Fukushima, S., Nishiyama, N., et al. (2011). In situ quantitative monitoring of polyplexes and polyplex micelles in the blood circulation using intravital real-time confocal laser scanning microscopy. *J Control Release, 151*, 104–109.

Oh, Y. K., & Park, T. G. (2009). SiRNA delivery systems for cancer treatment. *Advanced Drug Delivery Reviews, 61*, 850–862.

Owyong, M., Hosseini-Nassab, N., Efe, G., Honkala, A., van den Bijgaart, R. J. E., Plaks, V., et al. (2017). Cancer Immunotherapy Getting Brainy: Visualizing the Distinctive CNS Metastatic Niche to Illuminate Therapeutic Resistance. *Drug Resist Updat, 33-35*, 23–35.

Parker, N., Turk, M. J., Westrick, E., Lewis, J. D., Low, P. S., & Leamon, C. P. (2005). Folate receptor expression in carcinomas and normal tissues determined by a quantitative radioligand binding assay. *Analytical Biochemistry, 338*, 284–293.

Pommier, Y., Sordet, O., Antony, S., Hayward, R. L., & Kohn, K. W. (2004). Apoptosis defects and chemotherapy resistance: molecular interaction maps and networks. *Oncogene, 23*, 2934–2949.

Qu, D., Jiao, M., Lin, H., Tian, C., Qu, G., Xue, J., et al. (2020). Anisamide-functionalized pH-responsive amphiphilic chitosan-based paclitaxel micelles for sigma-1 receptor targeted prostate cancer treatment. *Carbohydr Polym, 229*, Article 115498.

Shahidi, F., & Synowiecki, J. (1991). Isolation and characterization of nutrients and value-added products from snow crab (Chionoecetes opilio) and shrimp (Pandalus borealis) processing discards. *Journal of Agricultural and Food Chemistry, 39*, 1527–1532.

Snyder, S., Murundi, S., Crawford, L., & Putnam, D. (2019). Enabling P-glycoprotein inhibition in multidrug resistant cancer through the reverse targeting of a quinidine-PEG conjugate. *Journal of controlled release : official journal of the Controlled Release Society, 317*, 291–299.

Wang, S., Liu, X., Chen, S., Liu, Z., Zhang, X., Liang, X. J., et al. (2019a). Regulation of Ca (2+) Signaling for Drug-Resistant Breast Cancer Therapy with Mesoporous Silica Nanocapsule Encapsulated Doxorubicin/siRNA Cocktail. *ACS nano, 13*, 274–283.

Wang, T., Luo, Y., Lv, H., Wang, J., Zhang, Y., & Pei, R. (2019b). Aptamer-Based Erythrocyte-Derived Mimic Vesicles Loaded with siRNA and Doxorubicin for the Targeted Treatment of Multidrug-Resistant Tumors. *ACS applied materials & interfaces, 11*, 45455–45466.

Wang, Y., Khan, A., Liu, Y., Feng, J., Dai, L., Wang, G., et al. (2019c). Chitosan oligosaccharide-based dual pH responsive nano-micelles for targeted delivery of hydrophobic drugs. *Carbohydr Polym, 223*, Article 115061.

Wise, J. G., Nanayakkara, A. K., Aljowni, M., Chen, G., De Oliveira, M. C., Ammerman, L., et al. (2019). Optimizing Targeted Inhibitors of P-Glycoprotein Using Computational and Structure-Guided Approaches. *Journal of medicinal chemistry, 62*, 10645–10663.

Xu, L., Bai, Q., Zhang, X., & Yang, H. (2017). Folate-mediated chemotherapy and diagnostics: An updated review and outlook. *Journal of controlled release : official journal of the Controlled Release Society, 252*, 73–82.

Yin, T., Liu, Y., Yang, M., Wang, L., Zhou, J., & Huo, M. (2020). Novel Chitosan Derivatives with Reversible Cationization and Hydrophobicization for Tumor Cytoplasm-Specific Burst Co-delivery of siRNA and Chemotherapeutics. *ACS Appl Mater Interfaces, 12*, 14770–14783.

Yuan, X., Peng, S., Lin, W., Wang, J., & Zhang, L. (2019). Multistage pH-responsive mesoporous silica nanohybrids with charge reversal and intracellular release for efficient anticancer drug delivery. *Journal of colloid and interface science, 555*, 82–93.

Zhao, Z., Ji, M., Wang, Q., He, N., & Li, Y. (2020). Ca(2+) signaling modulation using cancer cell membrane coated chitosan nanoparticles to combat multidrug resistance of cancer. *Carbohydr Polym, 238*, Article 116073.

Zheng, H., Tang, C., & Yin, C. (2015). Oral delivery of shRNA based on amino acid modified chitosan for improved antitumor efficacy. *Biomaterials, 70*, 126–137.

Zhu, H., Cao, X., Cai, X., Tian, Y., Wang, D., Qi, J., et al. (2019). Pifithrin-mu incorporated in gold nanoparticle amplifies pro-apoptotic unfolded protein response cascades to potentiate synergistic glioblastoma therapy. *Biomaterials, 232*, Article 119677.